Nonlinear behaviour and macroscopic strength of Flemish bond masonry

Matteo Bruggi and Alberto Taliercio*

Department of Civil and Environmental Engineering,
Politecnico di Milano,
P.za Leonardo da Vinci 32,
20133 Milan, Italy
Email: matteo.bruggi@polimi.it
Email: alberto.taliercio@polimi.it
*Corresponding author

Abstract: The prediction of the macroscopic behaviour of Flemish bond brickwork (FBB) is dealt with. From the finite element analysis of a representative volume element (RVE) of masonry, assumed to be a heterogeneous medium with periodic properties along two perpendicular directions, information on the macroscopic mechanical properties of masonry is obtained. The RVE is subjected to particular boundary conditions, which match the periodicity of the medium, to predict its response under elementary macroscopic stresses. The model takes into account the nonlinear behaviour of mortar and bricks by means of a combined plasticity and damage model. The macroscopic strength and post-peak behaviour of FBB under elementary in- and out-of-plane stresses are predicted. The biaxial macroscopic strength domain of masonry subjected to in-plane stress is also predicted for different orientations of the maximum principal stress to the bed joints.

Keywords: masonry; Flemish bond; homogenisation; damage; macroscopic strength.

Reference to this paper should be made as follows: Bruggi, M. and Taliercio, A. (xxxx) 'Nonlinear behaviour and macroscopic strength of Flemish bond masonry', *Int. J. Masonry Research and Innovation*, Vol. X, No. Y, pp.xxx–xxx.

Biographical notes: Matteo Bruggi is an Associate Professor of Structural Mechanics at Milan Technical University (Politecnico). He has authored nearly 130 papers on international journals, international and national conference proceedings, and book chapters. His fields of interest encompass structural optimisation, with emphasis on topology optimisation, and the equilibrium of structures that can be investigated using the elastic/rigid no-tension material model.

Alberto Taliercio is a Professor of Structural Mechanics at Milan Technical University (Politecnico). He has authored nearly 160 papers on international journals, international and national conference proceedings, and book chapters. His fields of interest encompass the modelling of the macroscopic behaviour of heterogeneous media (masonry, FRCs), structural optimisation, the study of the mechanical behaviour of quasi-brittle materials (concrete, masonry) under monotonic, cyclic, and sustained loads.

This paper is a revised and expanded version of a paper entitled 'Flemish bond brickwork: macroscopic elastic properties and nonlinear behaviour' presented at the 17th Int. Brick & Block Masonry Conf., Krakow, Poland, 5–8 July 2020.

1 Introduction

Flemish bond brickwork (FBB) is characterised by courses of units in which stretchers are alternated with headers. Headers are centred over the stretchers in the courses below, and connect the two wythes of stretchers effectively, thus providing FBB walls with a monolithic behaviour.

Flemish bond is extremely common in historical buildings (and beyond). Despite its diffusion, FBB has been addressed by a very limited number of authors, both from the experimental and the theoretical point of view. Indeed, a huge amount of papers exist addressing simpler brick patterns, such as running bond and header bond, which are characterised by homogeneous mechanical properties along the wall thickness. Interested readers are referred, e.g., to Pande et al. (1989), Cecchi and Sab (2002), Zucchini and Lourenço (2002), Mistler et al. (2007) and Taliercio (2014, 2016) as far as the prediction of the macroscopic elastic properties of masonry is concerned, and to Pietruszczak and Niu (1992), Milani (2011) and Milani and Taliercio (2015, 2016) as far as the modelling of the nonlinear behaviour and the macroscopic strength properties of masonry are concerned.

At the authors' knowledge, Drougkas et al. are the only researchers who have tried to predict the macroscopic mechanical properties of FBB. Assuming FBB to be a periodic, heterogeneous medium, these authors estimated the linear elastic properties of FBB by subdividing a representative element (RVE) in cubic sub-elements (Drougkas et al., 2015). By selecting suitable plasticity and damage models for mortar and units, they also predicted the nonlinear macroscopic stress-strain curves of FBB under uniaxial stress and the macroscopic strength domain of FBB under biaxial stresses parallel to the mortar joints (Drougkas et al., 2016).

Recently, Taliercio (2018) derived closed-form expressions for the macroscopic in-plane elastic constants and for the transverse shear moduli of FBB. An approach similar to the so-called Method of Cells proposed by Aboudi (1991) for fibre reinforced composites was used: any RVE is subdivided into sub-cells, and a piecewise differentiable, strain-periodic displacement field depending on a limited number of degrees of freedom (d.o.f.s) is formulated. Suitable equilibrium conditions at the interface between adjacent subcells reduce the number of independent d.o.f.s. Upon integration of the microscopic stress and strain fields, the macroscopic elastic constants can be identified.

Having reliable tools available to predict the macroscopic behaviour of masonry, including FBB, is of paramount importance in the analysis of large masonry buildings, for which a microscopic approach taking the heterogeneous nature of brickwork into account is impractical. In the present work, a numerical method suitable to describe the macroscopic nonlinear behaviour and the homogenised strength domain of FBB under any macroscopic stress conditions is presented, in order to contribute and fill the existing gap in this field.

Assuming FBB to be periodic, a finite element model of any RVE is analysed beyond the elastic limit. Suitable kinematic boundary conditions are enforced to match the strain-periodicity of the microscopic displacement field. The nonlinear mechanical behaviour and the development of cracks in units and mortar joints are described by the concrete damaged plasticity model, implemented in the FE commercial code Abaqus. The FE model is applied to predict the homogenised strength of FBB under elementary macroscopic in-plane stresses and transverse shear, assuming the units to be either weak or strong compared to mortar, in order to point out the change in macroscopic behaviour of masonry with the microscopic parameters. The effect of the collar joint on the macroscopic response is highlighted by comparing the numerical results with those obtained for header bond brickwork.

Under biaxial stresses, the strength domain and the elastic limit were evaluated at different orientations of the bed joints to the maximum principal stress; the results are qualitatively compared with those found in the literature for running bond masonry. Eventually, the main results of the research are critically discussed, and possible future perspectives of the research are outlined.

2 Numerical model

In this Section, the mathematical tools required to formulate the numerical model are summarised. First, some basic concepts of homogenisation theory for periodic media are recalled, and the periodicity conditions that the microscopic displacement field has to fulfil over any Representative Volume Element of FBB are shown (Section 2.1). Then, the constitutive law proposed for units and mortar in uniaxial tension or compression is described (Section 2.2), and the yield surface of the materials under 3D stress is outlined (Section 2.3).

2.1 Representative volume element of Flemish bond brickwork

Consider a typical masonry wall built using Flemish bond [Figure 1(a)]. From now onwards, x_1 and x_3 will denote a couple of axes parallel to the mid-plane of the wall, and x_2 an axis running across the wall thickness. Owing to the assumed periodicity, a single unit cell, V, can be used as RVE. For numerical purposes, only half of the RVE needs to be analysed and discretised into finite elements; in Figure 1(b), light elements correspond to mortar joints and dark elements to units.

Goal of homogenisation theory is replacing the real heterogeneous medium with a homogeneous material, and defining the homogenised, or macroscopic, properties though the analysis of any RVE. The homogenised constitutive law relates macroscopic stresses ($\boldsymbol{\Sigma}$) and macroscopic strains ($\boldsymbol{E}$), or their rates beyond the linear elastic field. $\boldsymbol{\Sigma}$ and $\boldsymbol{E}$ are defined as the volume averages of the corresponding microscopic fields, $\boldsymbol{\sigma}(\boldsymbol{x})$ and $\boldsymbol{\varepsilon}(\boldsymbol{x})$, over the volume, V, of the RVE, $\boldsymbol{x}$ being any point in V:

$$\boldsymbol{\Sigma} = \frac{1}{|V|}\int_V \boldsymbol{\sigma}(\boldsymbol{x})dV, \quad \boldsymbol{E} = \frac{1}{|V|}\int_V \boldsymbol{\varepsilon}(\boldsymbol{x})dV. \tag{1}$$

Further details on homogenisation theory for periodic media can be found, e.g., in Nemat-Nasser and Hori (1993).

Figure 1 (a) Typical Flemish bond brickwork (b) possible representative volume element (RVE) (see online version for colours)

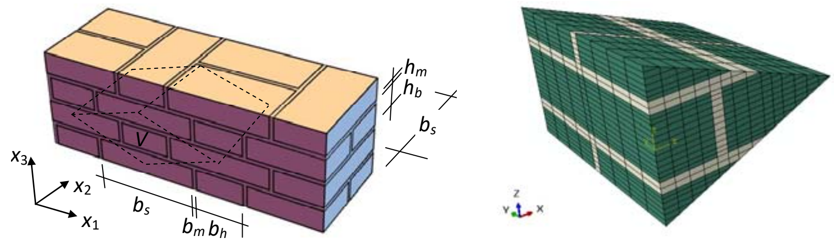

(a) (b)

According to Mistler et al. (2007), the (infinitesimal) microscopic displacement field in the RVE of any periodic, heterogeneous body can be expressed as:

$$\boldsymbol{u}(\boldsymbol{x}) = \boldsymbol{u}_0 + \boldsymbol{\Omega} \wedge x + \tilde{\boldsymbol{E}}\boldsymbol{x} + \boldsymbol{u}^p(\boldsymbol{x}), \tag{2}$$

where $\boldsymbol{u}_0$ is a rigid displacement, $\boldsymbol{\Omega}$ is a rigid rotation, and up is the periodic part of the displacement field: up matches the periodicity of the medium along x_1 and x_3. $\tilde{\boldsymbol{E}}$ is the extensive variable conjugate to the macroscopic stress in the so-called Hill's macro-homogeneity:

$$\boldsymbol{\Sigma} : \tilde{\boldsymbol{E}} = \frac{1}{|V|}\int_V \boldsymbol{\sigma}(\boldsymbol{x}) : \varepsilon(\boldsymbol{x}) dV \tag{3}$$

and differs from the macroscopic strain $\boldsymbol{E}$ unlike the case of fully periodic media (Nemat-Nasser and Hori, 1993). Equation (3) applies provided that the microscopic stress field is anti-periodic in (x_1, x_3) over the boundary of the RVE in contact with the surrounding RVEs, whereas the faces perpendicular to x_2 are traction-free.

A microscopic displacement field of the form (2) over the RVE is said to be 'strain-periodic'.

Any macroscopic strain or stress can be prescribed by applying suitable boundary conditions, in terms of displacements or forces, respectively. Interested readers are referred to Mistler et al. (2007) for further details.

2.2 Constitutive law of units and joints

In the numerical applications, the nonlinear behaviour of units and mortar is described by the so-called 'concrete damaged plasticity' (hereafter, CDP) model implemented in Abaqus. This model takes into account both plastic strains and damage, and was successfully used by other authors to analyse masonry buildings under seismic actions (Milani and Valente, 2015; Valente and Milani, 2016; Condoleo et al., 2020). The CDP model is only briefly described hereafter: readers are referred to the Abaqus Theory Manual for additional details.

Figure 2 Stress-strain curves (blue) and damage evolution (red) in tension (d_t) and compression (d_c) for (a, b) weak units, (c, d) strong units and (e, f) mortar (see online version for colours)

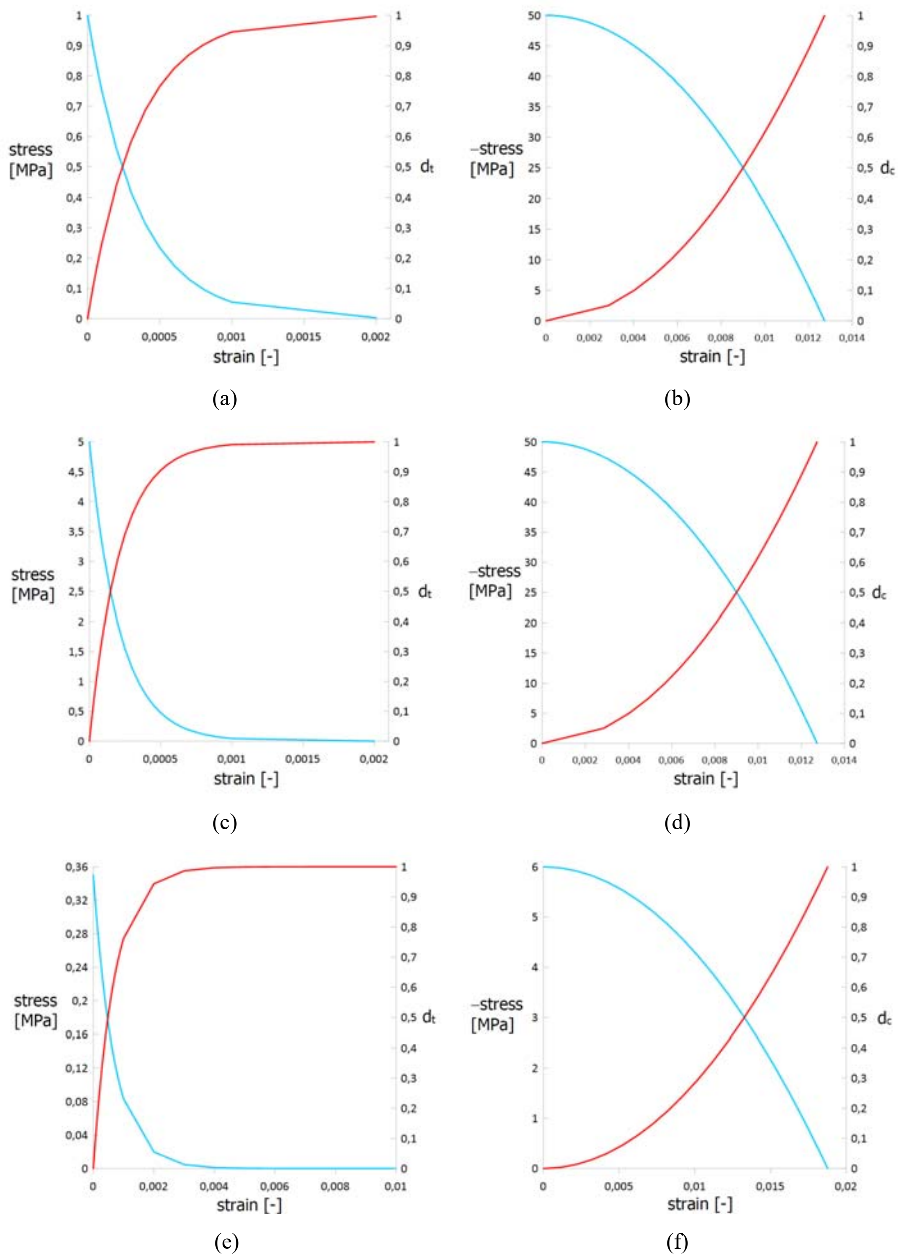

The model makes use of the concept of 'effective stress' to define the stress-strain relations, both in tension and compression:

$$\bar{\sigma} = \frac{\sigma_h}{1 - d_h}, \tag{4}$$

where $h = t$ for tension and $h = c$ for compression. The damage variables in tension and compression are denoted by d_t and d_c, respectively. Figure 2 summarises the post-peak stress-strain curves assumed in the numerical analyses for weak units [Figures 2(a) and 2(b)], strong units [Figures 2(c) and 2(d)] and mortar [Figures 2(e) and 2(f)], both in tension [Figures 2(a), 2(c) and 2(e)] and compression [Figures 2(b), 2(d) and 2(f)]. The same figures also show the assumed evolution of dt and dc as strain increases.

Two different brick types were considered in the applications, namely bricks having a tensile strength comparable to that of mortar ('weak' units), and bricks having a tensile strength of an order of magnitude greater than that of mortar ('strong' units). The values of the uniaxial tensile (σ_{t0}) and compressive (σ_{c0}) strength of bricks and mortar are listed in Table 1.

Table 1 Uniaxial tensile and compressive strength of units and mortar

Material	σ_{t0}	σ_{c0}
	N/mm^2	N/mm^2
Weak units	1	50
Strong units	5	
Mortar	0.35	6

The tensile behaviour of bricks and mortar is assumed to be linearly elastic up to σ_{t0}. Then microcracking occurs, and the material exhibits strain softening behaviour. The blue curves in Figures 2(a), 2(c) and 2(e) show the assumed post-peak behaviour in tension for weak units, strong units, and mortar, respectively. Basically, an exponential softening is assumed.

Conversely, in compression the assumed post-peak behaviour of the component materials is shown in Figures 2(b), 2(d) and 2(f) for weak units, strong units, and mortar, respectively. A sort of parabolic softening is prescribed.

2.3 Multiaxial nonlinear behaviour

Under multiaxial stresses, the yield surface implemented in the CDP model is a modified Drucker-Prager surface, with a smoothed tip and a non-circular cross-section in the space of the principal stresses. A non-associated plastic flow rule, defined by a dilation angle ψ, is assumed. The values of the parameters that define the CDP model are summarised in Table 2; the same values were used for both mortar and units, irrespective of the strength of the units. The 'eccentricity' ε is a small positive number related to the flow potential. σ_{b0} is initial yield stress in biaxial compression when the two principal stresses are equal. K_c defines the shape of the cross-section of the yield surface in a plane perpendicular to the hydrostatic axis. The parameter μ is introduced for the visco-plastic regularisation of the constitutive equations. Readers are referred to the Abaqus Theory Manual (2006) for additional details.

Table 2 Parameters defining the CDP model used in the numerical applications

ψ *(deg)*	ε	σ_{b0}/σ_{c0}	K_c	μ
10	0.1	1.16	2/3	0.0001

3 Macroscopic behaviour under elementary macroscopic stress

The results of numerical tests on RVEs subjected to selected elementary macroscopic stresses will be now shown and discussed in terms of macroscopic stress-strain curves and contours of the damage variables at the last increments of the numerical analyses, when a failure mechanism is apparent. In order to highlight the influence of the collar joint on the macroscopic response of masonry, the results are compared with those obtained on RVEs of Header Bond Brickwork (HBB) having the same geometrical and mechanical properties as FBB.

3.1 Vertical compression ($\Sigma_{33} < 0$)

Masonry walls are mainly supposed to withstand vertical loads. Thus, it is of particular interest to investigate the behaviour of masonry (namely, its load-bearing capacity) under vertical compression, Σ_{33}. Figure 3 shows the macroscopic stress-strain curves obtained for FBB and HBB assuming the units to be either weak [Figure 3(a)] or strong [Figure 3(b)]. Unsurprisingly, the macroscopic strength is similar for both bonds, as the vertical joints do not contribute to the vertical strength significantly. The post-peak behaviour of FBB and HBB is somewhat different, although the ultimate behaviour is similar. If the units are weak, tensile damage is mainly located in the vertical (head and collar) joints in both bonds [Figures 4(a) and 4(b)], but headers are also damaged in FBB. If the units are strong, they turn out to be heavily damaged in tension in both bonds [Figures 4(c) and 4(d)]. Compressive damage is basically located in the bed joints, for both bonds and irrespective of the strength of the units (Figure 5).

Figure 3 Macroscopic stress-strain curves for FBB and HBB under vertical compression, (a) weak units (b) strong units (see online version for colours)

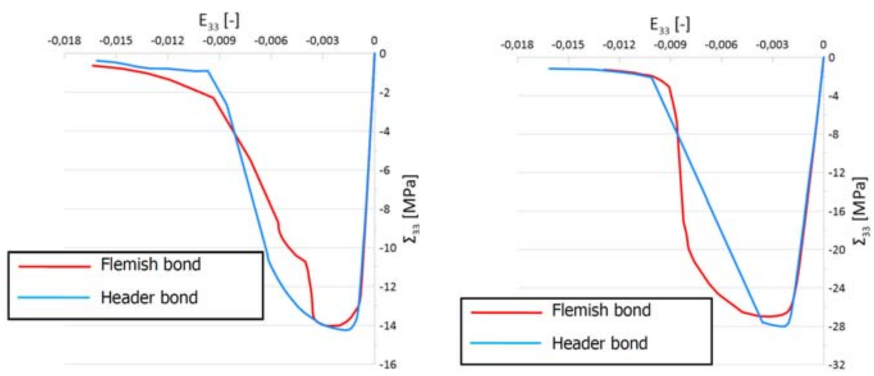

(a) (b)

Figure 4 Ultimate contours of tensile damage for (a, c) Flemish bond and (b, d) header bond brickwork under vertical compression, (a, b) weak units (c, d) strong units (see online version for colours)

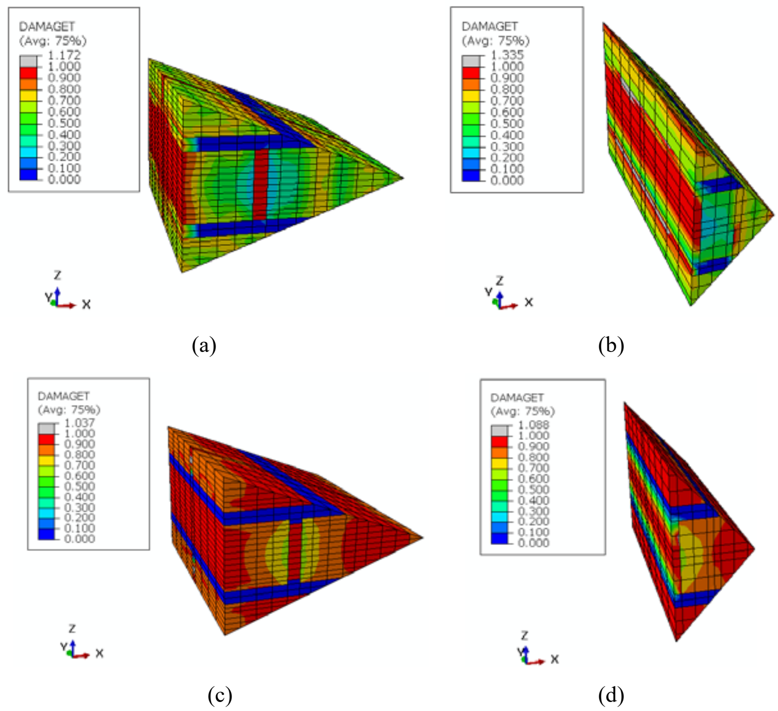

Figure 5 Ultimate contours of compression damage for (a, c) Flemish bond and (b, d) header bond brickwork under vertical compression, (a, b) weak units (c, d) strong units (see online version for colours)

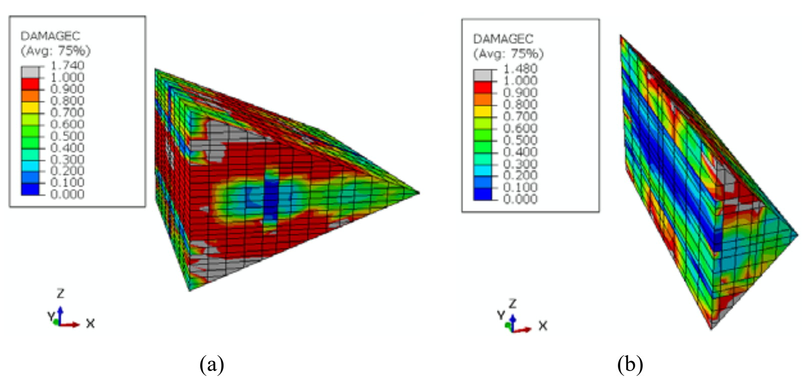

Figure 5 Ultimate contours of compression damage for (a, c) Flemish bond and (b, d) header bond brickwork under vertical compression, (a, b) weak units (c, d) strong units (continued) (see online version for colours)

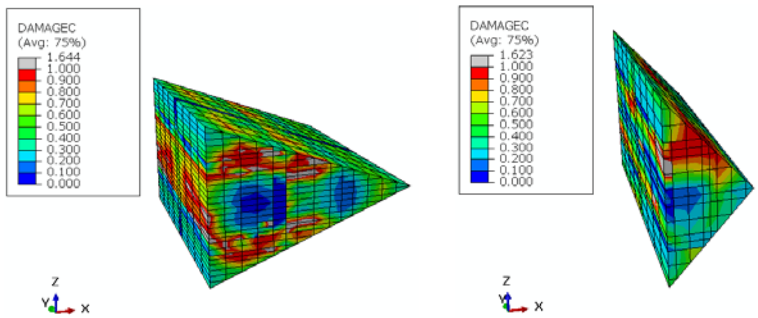

(c) (d)

3.2 Horizontal tension ($\Sigma_{11} > 0$)

Under horizontal tension, the two bonds have the same macroscopic strength if units are weak [Figure 6(a)]. Indeed, tensile damage is localised in the bed and head joints [Figures 7(a) and 7(b); the occurrence of tensile damage also in the stretchers of FBB explains the difference in post-peak behaviour of the two bonds [Figures 6(a)]. If units are strong, FBB exhibits a macroscopic strength much higher than HBB [Figure 6(b)], although the ultimate damage distribution is similar [Figure 7(c) and 7(d)]. The higher tensile strength of the units prevents stretchers from cracking, whereas the failure mechanism of HBB is basically the same, irrespective of the brick strength. Note that collar joints are undamaged in FBB under horizontal tension.

Figure 6 Macroscopic stress-strain curves for FBB and HBB under horizontal tension, (a) weak units (b) strong units (see online version for colours)

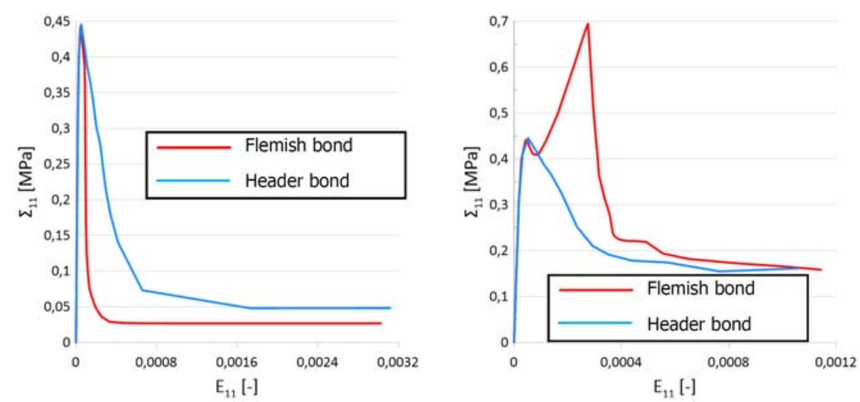

(a) (b)

Figure 7 Ultimate contours of tensile damage for (a, c) Flemish bond and header (b, d) bond brickwork under horizontal tension, (a, b) weak units (c, d) strong units (see online version for colours)

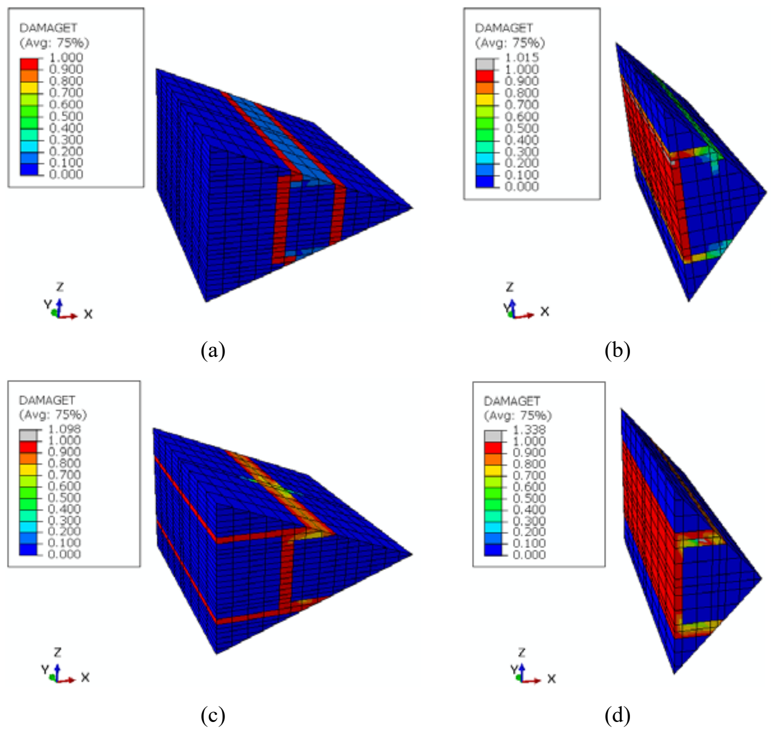

Figure 8 Macroscopic stress-strain curves for FBB and HBB under in-plane shear, (a) weak units (b) strong units (see online version for colours)

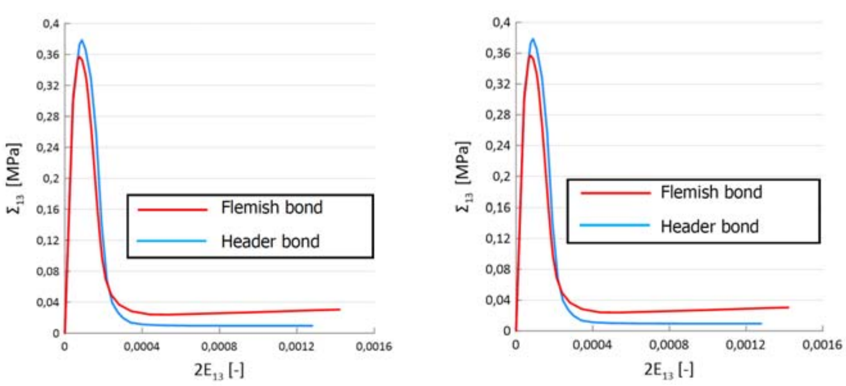

(a) (b)

3.3 In-plane shear (Σ_{13})

Under in-plane shear, neither the brick strength nor the brick pattern affects the macroscopic behaviour of masonry significantly. Figure 8 shows the macroscopic stress-strain curves for weak units [Figure 8(a)] and strong units [Figure 8(b)]. The difference in behaviour is barely perceptible. Indeed, damage evolution is basically the same in FBB and HBB, irrespective of the brick strength, as it basically affects only head and bed joints (Figure 9).

Figure 9 Ultimate contours of tensile damage for (a, c) Flemish bond and (b, d) header bond brickwork under in-plane shear, (a, b) weak units and (c, d) strong units (see online version for colours)

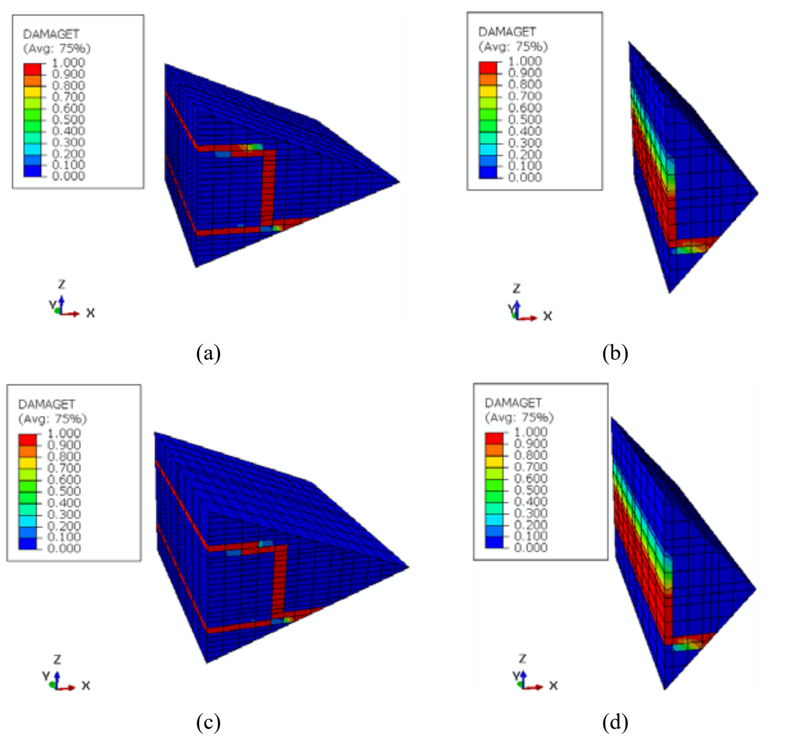

Similar remarks apply to the macroscopic behaviour under vertical transverse shear (Σ_{23}), both in terms of macroscopic strength and damage evolution. In this case, only the bed joints are significantly affected by damage.

3.4 Horizontal transverse shear (Σ_{12})

Finally, in the case of horizontal shear both the macroscopic strength and the macroscopic nonlinear behaviour are significantly affected by the type of bond and the brick strength. Figure 10(a) shows that if units are weak the macroscopic shear strength of FBB is significantly lower than that of HBB. This can be easily understood referring to

Figure 11, where the contours of the ultimate tensile damage and the failure mechanism are shown. In FBB, damage occurs in the collar joint and then propagates in the weak units [Figure 11(a)]: the ultimate behaviour of the RVE is basically that of two rigid elements undergoing a relative sliding [Figure 11(c)]. The absence of any collar joint enhances the strength of HBB.

Conversely, if units are strong damage is mostly confined in the bed and head joints, both in FBB and in HBB (Figure 12). The collar joint is affected by damage only to a limited extent, and the macroscopic strength of FBB is higher than that of HBB [Figure 10(b)].

Figure 10 Macroscopic stress-strain curves for FBB and HBB under horizontal transverse shear, (a) weak units (b) strong units (see online version for colours)

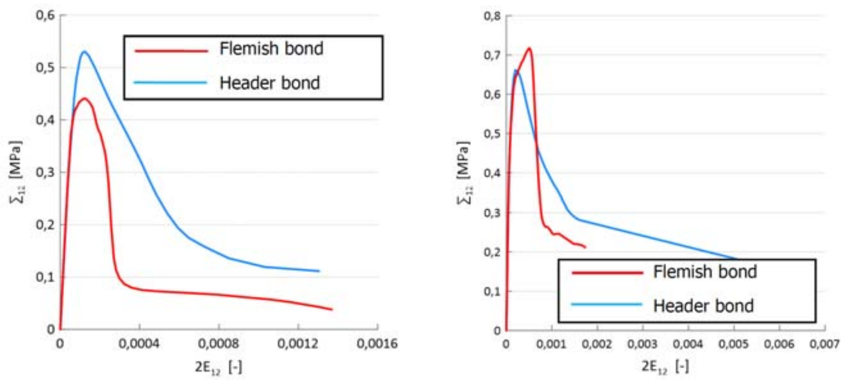

(a) (b)

Figure 11 Brickwork with weak units under horizontal transverse shear: ultimate contours of (a, b) tensile damage and (c, d) failure mechanisms for (a, c) Flemish bond and (b, d) header bond (see online version for colours)

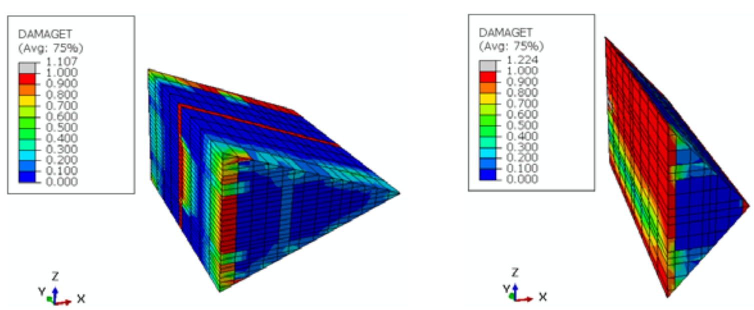

(a) (b)

Figure 11 Brickwork with weak units under horizontal transverse shear: ultimate contours of (a, b) tensile damage and (c, d) failure mechanisms for (a, c) Flemish bond and (b, d) header bond (continued) (see online version for colours)

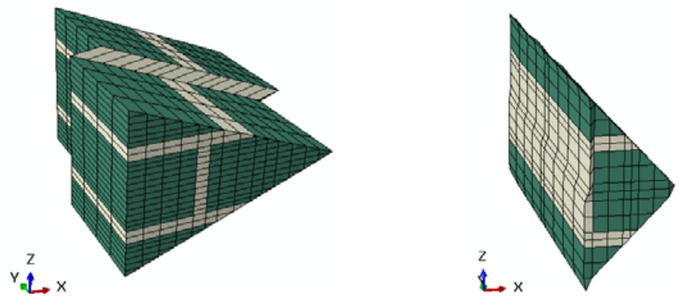

(c) (d)

Figure 12 Brickwork with strong units under horizontal transverse shear: ultimate contours of (a, b) tensile damage and (c, d) failure mechanisms for (a, c) Flemish bond and (b, d) header bond (see online version for colours)

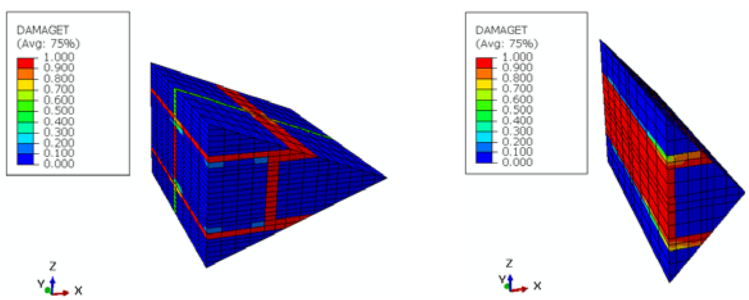

(a) (b)

(c) (d)

4 Homogenised biaxial strength

The homogenised biaxial strength of FBB was predicted by submitting any RVE to in-plane macroscopic stresses, Σ_I and Σ_{II}. The orientation, θ, of the maximum principal stress to the bed joints was assumed to range from 0 to 90°, with a step of 22.5°. Radial stress paths were followed in the plane (Σ_I, Σ_{II}): the macroscopic strength domain was obtained as the envelope of the stress points at the last increment of the analysis for each stress path. The mechanical properties of the component materials are those listed in Table 1 for strong units. The results obtained for weak units are not presented hereafter, for the sake of brevity; where appropriate, comments on the influence of the unit strength on the macroscopic strength will be added.

Figure 13(a) shows the failure surfaces obtained according to the procedure outlined above. Apparently, the numerical model is capable of capturing the macroscopically anisotropic behaviour of brickwork. At a given orientation θ, under biaxial compression the macroscopic strength is affected at a limited extent by the ratio of the two principal stresses: conversely, there is a significant increase in strength from uniaxial to biaxial compression. Note that all the failure surfaces referred to different orientations are supposed to intersect at the same point under equi-biaxial compression (or tension): this requirement is not rigorously fulfilled in Figure 13a because of the difficulty in identifying macroscopic failure numerically.

In Figure 13(b), the elastic domains of FBB at different orientations are shown. For each orientation, the elastic domain was numerically identified as the envelope of the macroscopic stress points at which damage was found to occur in the RVE. At a given θ, it is interesting to note that the elastic domain is not a simple homothetic contraction of the corresponding strength domain.

Figure 13 (a) Macroscopic strength domains and (b) elastic domains at different orientations (θ) of the maximum principal stress to the bed joints (see online version for colours)

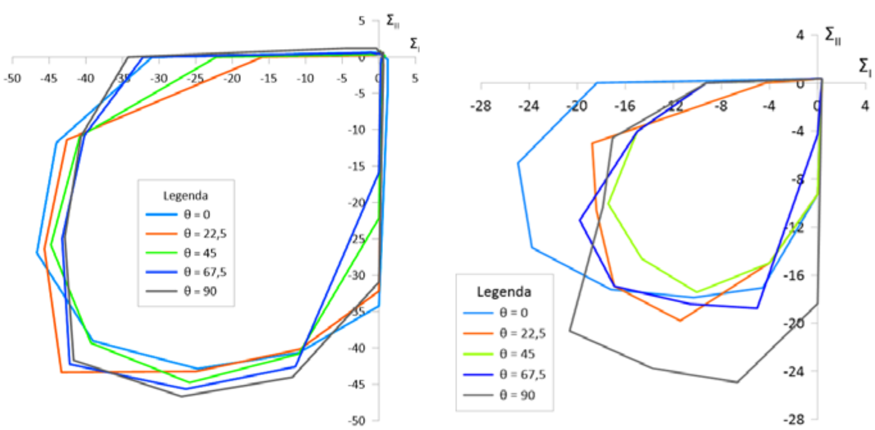

(a) (b)

Unfortunately, the validation of the numerical model cannot be done by comparison with experimental data, because of their unavailability in the current literature. A qualitative assessment of the model can be done referring to the data of tests on single-wythe masonry. Figure 14(a) shows the bounds of the experimental biaxial strength of running bond masonry subjected to biaxial tests assuming the macroscopic principal stresses to be parallel to the bed and head joints, reported by Drougkas et al. (2016). For comparison, also the theoretical strength domain numerically obtained by these authors is shown. Figure 14b shows the strength envelope obtained by the proposed numerical model at $\theta = 0°$. Experimental and numerical results are in qualitative good agreement, although a quantitative comparison cannot be done. In Figure 14(b), also the elastic domain of FBB at $\theta = 0°$ is shown.

Figure 14 Biaxial stresses acting parallel to the bed and head joints ($\theta = 0°$), (a) experimental strength domain of running bond masonry, compared with the theoretical predictions of Drougkas et al. (2016) (b) numerical strength domain and elastic domain of FBB

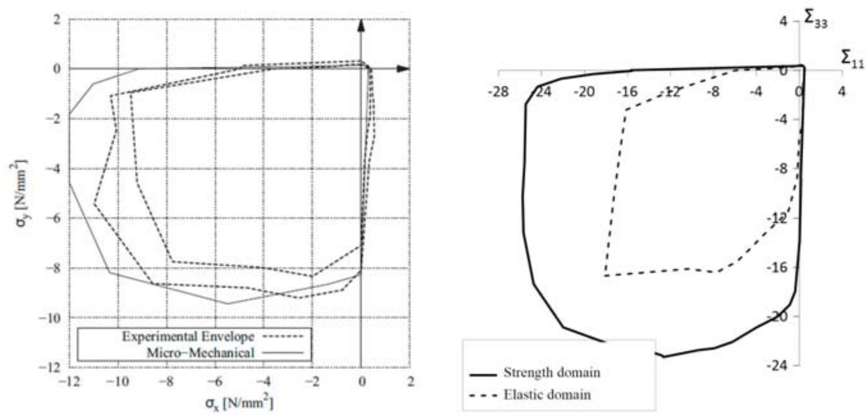

(a) (b)

Another possibility to qualitatively assess the numerical results is to compare the failure mechanisms of FBB predicted by the FE model with those reported by other authors for single-wythe masonry. Figure 15 summarises the numerical failure mechanisms, as suggested by the ultimate contours of the damage variables, at different combinations of the macroscopic and orientations of the macroscopic principal stresses. All of these mechanisms are in good agreement with those reported by Dhanasekar et al. (1985) for stretcher bond brickwork: readers are referred to the original paper for additional details. Note that under biaxial compression failure is invariably associated with splitting at the wall mid-plane, both for stretcher bond and Flemish bond masonry. For FBB, this is shown in Figure 16, where the contours of the tensile damage variable at the last increment of the analyses are shown under biaxial compression at $\theta = 45°$ for a selected ratio of the principal stresses. Apparently, damage is localised in the collar joints, whereas the remaining joints are undamaged. Similar remarks apply to FBB with weak units.

Figure 15 Numerically identified failure mechanisms of FBB under different stress combinations (see online version for colours)

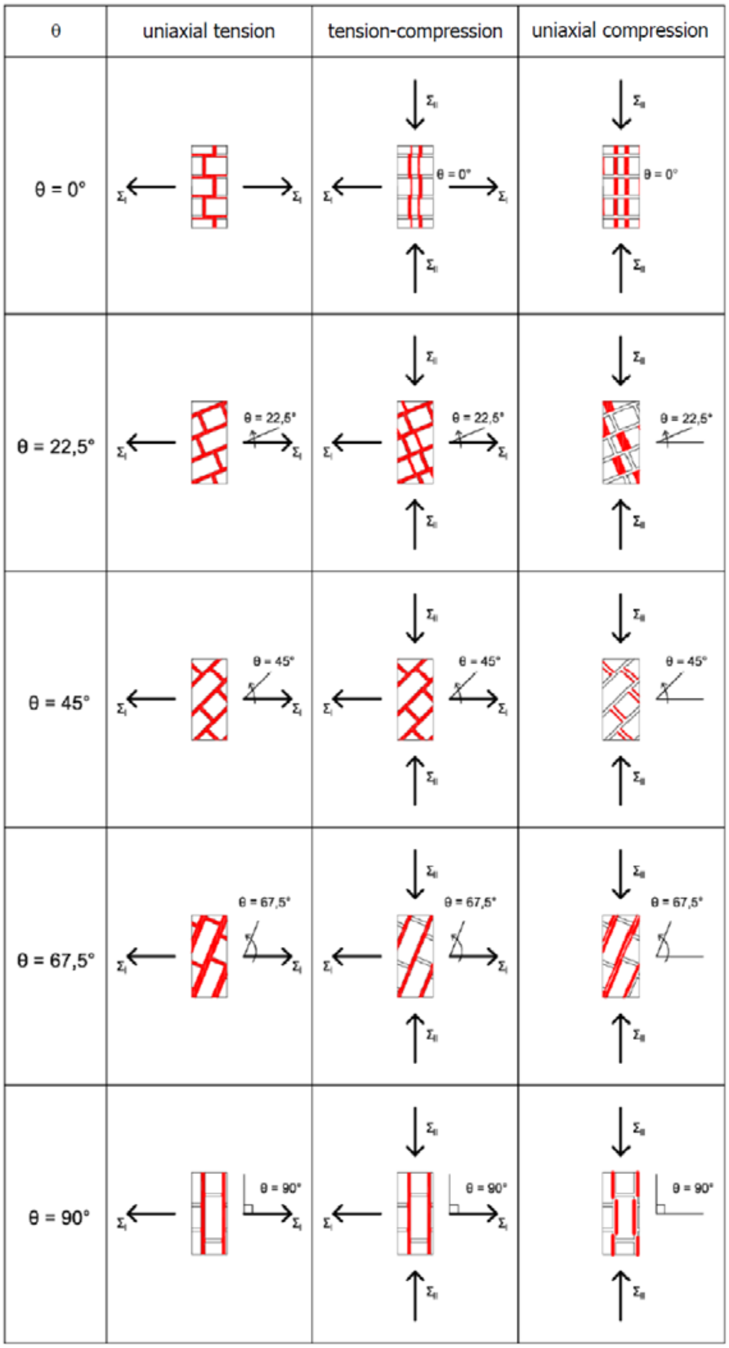

Figure 16 Ultimate contours of tensile damage at failure in biaxial compression (θ= 45°) (see online version for colours)

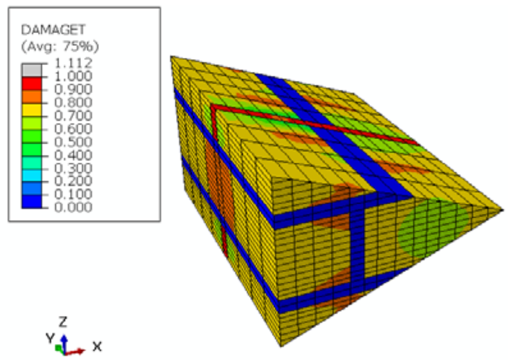

The difference in ultimate behaviour explains the difference in macroscopic strength as the orientation of the principal stresses varies. Figure 17 shows the contours of the tensile damage variable at the last increment of the numerical analyses under vertical tension (θ = 90°); basically, only the bed joints are damaged. The macroscopic strength is 0.4 N/mm^2 approximately. Comparing this picture to Figure 7(c), which refers to horizontal tension (θ= 0°), it is easy to understand why the macroscopic tensile strength is much higher in the latter case (0.7 N/mm^2 approximately). This result is in agreement with the experimental findings obtained by Johnson and Thompson (1969) and by Page (1982). For FBB with weak units, anisotropy in terms of macroscopic tensile strength is significantly lower.

Figure 17 Contours of tensile damage at failure in uniaxial vertical tension (θ = 90°) (see online version for colours)

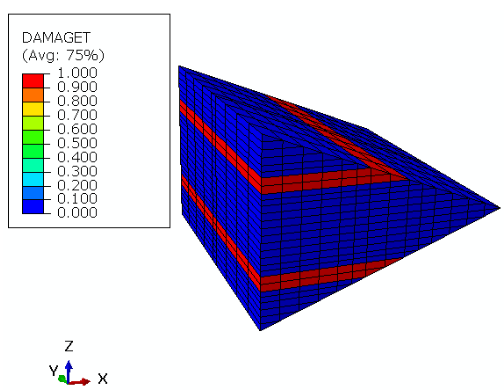

It was already remarked that a lateral confinement increases the compressive strength with respect to the uniaxial compressive strength. The increase is particularly significant at θ = 67.5° [see Figure 13(a). Figure 18 shows the contours of the tensile damage at failure under uniaxial compression [Figure 18(a)[and biaxial compression [Figure 18(b)]. Damage is much more widespread under uniaxial compression, as also the bed joints and parts of the units are damaged. Under biaxial compression, damage is basically confined within the collar joint (see also Figure 16). Similar remarks apply at any θ.

Figure 18 Contours of the tensile damage at failure at $\theta = 67.5°$, (a) uniaxial compression (b) biaxial compression (see online version for colours)

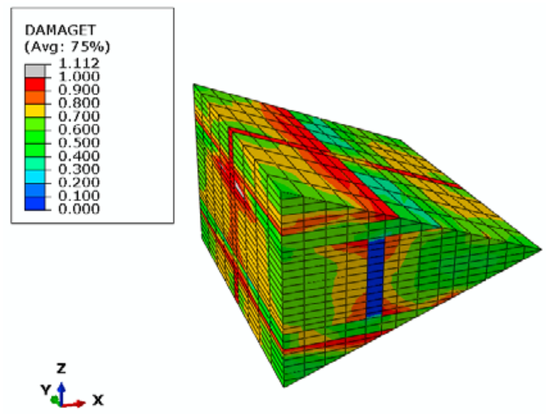

(a)

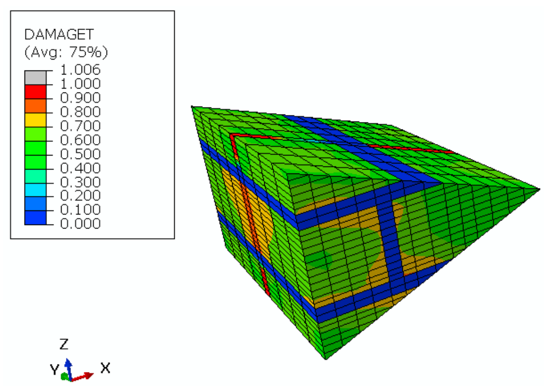

(b)

5 Concluding remarks

The proposed numerical model allows the macroscopic strength properties of FBB to be predicted and compared with those of other bonds (i.e. header or stretcher bond) in which no collar joint exists. Also, the influence of the microscopic mechanical properties on the homogenised nonlinear properties can be investigated.

Flemish bond and header bond exhibit similar macroscopic behaviour under vertical compression ($\Sigma_{33} < 0$), in-plane shear (Σ_{13}), and vertical transverse shear ($\Sigma_{23} < 0$). Under horizontal tension ($\Sigma_{11} > 0$), the two bonds behave similarly if units are weak. Increasing the tensile strength of the units, the macroscopic tensile strength increases only for FBB, as the failure mechanism of header bond in horizontal tension affects only the mortar joints.

The two bonds behave quite differently under horizontal transverse shear (Σ12). FBB has a strength higher than header bond owing to the presence of headers and stretchers in the same course. For both bonds, an increase in tensile strength of the units is matched by an increase in macroscopic shear strength.

Table 3 summarises the results of the numerical tests in terms of macroscopic strength under elementary stresses.

Table 3 Macroscopic strength (in N/mm^2) under elementary stresses for Flemish and header bond brickwork with weak and strong units

Unit strength	*Bond type*	Σ_{11} *(>0)*	Σ_{33} *(<0)*	Σ_{33} *(<0)*	Σ_{33} *(<0)*	Σ_{33} *(<0)*
Weak Units	HBB	0.445	14.25	0.379	0.398	0.53
	FBB	0.443	14.03	0.357	0.389	0.441
Strong Units	HBB	0.445	28.01	0.374	0.398	0.662
	FBB	0.695	26.99	0.355	0.396	0.718

Under biaxial compression, damage is localised in the collar joint, so that the macroscopic strength is nearly unaffected by the tensile strength of the units. This failure mechanism is similar to that reported by Page (1981) from tests on running bond brickwork.

The effectiveness of the numerical model needs to be validated by experimental tests. Unfortunately, in the available literature no results of tests on FBB specimens are reported. An extensive experimental program aimed at investigating the behaviour of FBB under different stress conditions is highly desirable to fill the existing knowledge gap on this very common type of masonry. It will probably take years to be carried out, and involve multiple research laboratories. Thus, the presented work is meant to be an initial, but certainly not exhaustive step, for a better understanding of the influence of the mechanical properties of mortar and units on the global behaviour of FBB.

Acknowledgements

The authors are indebted to Dr Fatima Midali, who carried out and processed the numerical analyses. The authors gratefully acknowledge the financial support of the Italian Ministry of Education University and Research 2015JW9NJT.

References

Abaqus (2006) *Finite Element Analysis (Theory Manual)*, Dassault Systèmes Simulia Corporation, Providence, RI (USA).

Aboudi, J. (1991) 'Mechanics of composite materials – a unified micromechanical approach', *Studies in Applied Mechanics*, Vol. 29, Elsevier, Amsterdam.

Cecchi, A. and Sab, K. (2002) 'A multi-parameter homogenization study for modeling elastic masonry', *Eur. J. Mech. A/Solids*, Vol. 21, No. 2, pp.249–268.

Condoleo, P., Gobbo, A. and Taliercio, A. (2020) 'A hybrid masonry and steel mirror-type vault with lunettes: survey and structural analysis', *Int. J. Arch. Herit.*, Vol. 14, No. 4, pp.496–516.

Dhanasekar, M., Page, A.W. and Kleeman, P.W. (1985) 'The failure of brick masonry under biaxial stresses', *Proc. Instn. Civ. Engrs. Part 2*, Vol. 79, pp.295–313.

Drougkas, A., Roca, P. and Molins, C. (2015) 'Analytical micro-modeling of masonry periodic unit cells - Elastic properties', *Int. J. Solids Struct.*, Vols. 69–70, pp.169–188.

Drougkas, A., Roca, P. and Molins, C. (2016) 'Nonlinear micro-mechanical analysis of masonry periodic unit cells', *Int. J. Solids Struct.*, Vol. 80, pp.193–211.

Johnson, F.B. and Thompson, J.N. (1969) 'Development of diametral testing procedures to provide a measure of strength characteristics of masonry assemblages', in Johnson, F.B. (Ed.): *Designing, Engineering and Construction with Masonry Products*, pp.51–57, Gulf Publishing Co., Houston, TX (USA).

Milani, G. (2011) 'Simple homogenization model for the non-linear analysis of in-plane loaded masonry walls', *Comput. Struct.*, Vol. 89, Nos. 17–18, pp.1586–1601.

Milani, G. and Taliercio, A. (2015) 'In-plane failure surfaces for masonry with joints of finite thick-ness estimated by a method of cells-type approach', *Comput. Struct.*, Vol. 150, pp.34–51.

Milani, G. and Taliercio, A. (2016) 'Limit analysis of transversally loaded masonry walls using an innovative macroscopic strength criterion', *Int. J. Solids Struct.*, Vol. 81, pp.274–293.

Milani, G. and Valente, M. (2015) 'Failure analysis of seven masonry churches severely damaged during the 2012 Emilia-Romagna (Italy) earthquake: non-linear dynamic analyses vs conventional static approaches', *Eng. Fail. Analysis*, Vol. 54, pp.13–56.

Mistler, M., Anthoine, A. and Butenweg, C. (2007) 'In-plane and out-of-plane homogenisation of masonry', *Comput. Struct.*, Vol. 85, Nos. 17–18, pp.1321–1330.

Nemat-Nasser, S. and Hori, M. (1993) *Micromechanics: Overall Properties of Heterogeneous Materials*, North-Holland, London.

Page, A.W. (1981) 'The biaxial compressive strength of brick masonry', *Proceedings of the Institution of Civil Engineers Part 2*, Vol. 71, pp.893–906.

Page, A.W. (1982) 'An experimental investigation of the biaxial strength of brick masonry', *Proceedings of the 6h Brick Masonry Conference*, Rome, Italy, pp.3–15.

Pande, G.N., Liang, J.X. and Middleton, J. (1989) 'Equivalent elastic moduli for brick masonry', *Comput. Geotech.*, Vol. 8, No. 3, pp.243–265.

Pietruszczak, S. and Niu, X. (1992) 'A mathematical description of macroscopic behaviour of brick masonry', *Int. J. Solids Struct.*, Vol. 29, No. 5, pp.531–546.

Taliercio, A. (2014) 'Closed-form expressions for the macroscopic in-plane elastic and creep coefficients of brick masonry', *Int. J. Solids Struct.*, Vol. 51, No. 17, pp.2949–2963.

Taliercio, A. (2016) 'Closed-form expressions for the macroscopic flexural rigidity coefficients of periodic brickwork', *Mech. Res. Comm.*, Vol. 72, pp.24–32.

Taliercio, A. (2018) 'Closed-form expressions for the macroscopic elastic constants of Flemish Bond masonry walls', *Proceedings of the 10th International Masonry Conference*, 9–11 July, Milan, Italy, pp.1721–1731.

Valente, M. and Milani, G. (2016) 'Seismic assessment of historical masonry towers by means of simplified approaches and standard FEM', *Const. Build. Mat.*, Vol. 108, pp.74–104.

Zucchini, A. and Lourenço, P.B. (2002) 'A micro-mechanical model for the homogenization of masonry', *Int. J. Solids Struct.*, Vol. 39, No. 12, pp.3233–3255.